Presented at the Research Congress 2013
De La Salle University Manila
March 7-9, 2013

EVALUATION OF SUPER-RESOLUTION METHODS FOR LOW-RESOLUTION IMAGE ENHANCEMENT

Joshua Jorel T. Lee, Aaron Spencer K. Ngo, Sherwin Victor S. Que and Ana Marian M. Pedro
Center for Automation Research, CCS DLSU-Manila 2401 Taft Ave, Manila, Philippines

Abstract: Super-resolution is a technique wherein a low-resolution image is enhanced to form a comprehensible image. It is done by either classical mathematical interpolation, combination/reconstruction or example based learning algorithms. One of the major challenges of super-resolution is acquiring an accurate image registration of an image set and performing the necessary image reconstruction algorithms. In this paper, we discuss the image registration algorithm performed by Vandewalle et al. and evaluate three image reconstruction algorithms that use image combination and classical super resolution techniques based on their resulting SNR and image quality. A survey of 25 people was performed in order to evaluate the image quality of each algorithm. Results of the survey established that among the three, the normalized convolution performed best followed by bi-cubic interpolation and the theory of Projections Onto Convex Sets (POCS). However, objective testing showed that SNR values vary slightly with standard deviations ranging from 0.04 to 4.32.

Key words: Image Processing; Image Resolution

1. INTRODUCTION

Every digitized picture has a set image resolution. The higher the image resolution, the higher its resolving power, which is the amount of details present in the image. In order to create a high-resolution image, multiple low-resolution pictures may be used in conjunction with super-resolution algorithms.

Super-resolution techniques combine the details found in multiple low-resolution pictures, of the same scene, and from this, a higher-resolution image may be derived. Normally when images are magnified, the quality degrades since the image does not contain enough information to display the enlarged content. Aliasing of images also occurs when trying to increase the size of an image. Super-resolution algorithms are performed in order to preserve the quality of such an image. Through the use of this technique, the low-resolution image may be magnified several times while containing the same details as the original picture.

Using super-resolution is highly desirable in cases where image detail is imperative. One such application is in satellite imagery wherein images are magnified in order to acquire a basic idea of the area or location. By applying super-resolution techniques, enlarged images may still retain significant details. NASA also implores the use of super-resolution techniques to further aid their research in space and aeronautics. Super-resolution also has applications in forensic imaging. Details from crime scenes can be further analysed away from the area due to the resulting enhanced images. Medical sciences may also use super-resolution in applications such as x-ray image enhancement.

This paper discusses image registration through the frequency domain and evaluate three image reconstruction algorithms. Testing and evaluation is done both objectively and subjectively. Objective testing was done by computing for the SNR of the generated image and the original image and subjective testing was done by conducting a survey of 25 people that required them to rate the output image of each of the three image reconstruction algorithms purely from the appearance of each image.

2. SUPER-RESOLUTION

Super-resolution algorithms typically involve the use of single or multiple low-resolution images in order to reconstruct the same image with a higher resolution.

One of the major challenges in super-resolution is determining the differences between the set of low-

resolution images. Differences may include camera motion, change of focus or both and the like. It is imperative to be able to precisely estimate the motion between the images since an error in estimation almost always translates to the degradation of the high-resolution image. The process for aligning the set of low-resolution images for super-resolution is called image registration.

A. Image Registration

Precise subpixel image registration is a basic requirement for good image reconstruction [7]. Inaccurately registering the images would not yield a good representation of the original signal. Registration may be done in either the frequency or spatial domain. In this study, image registration is done by using a frequency domain approach by [7].

Frequency domain methods consider only planar shifts and possible planar rotations. These are easily expressed in the Fourier domain. Furthermore, aliasing is also easier to identify and handle in the frequency domain. It must be noted that most frequency domain registration methods rely on the fact that shifted images differ in the frequency domain by a phase shift found in their correlation.

Vandewalle et al. uses a frequency domain algorithm that registers not just low-resolution images, but as well as aliased images. The algorithm makes use of a planar motion model because of the assumption that when a series of images is taken in a short amount of time, the images only experience a small amount of movement. Moreover, a planar motion model is simpler and has less parameters, which makes it more robust to noise.

Their algorithm starts by computing the Fourier transform of the low-resolution images, then performing their modified rotation estimation and shift estimation algorithms. Further discussion on the theories behind the frequency domain approach of Vandewalle et al. can be found in [7].

B. Image Reconstruction

Once accurate image registration has been performed, the samples from the different images in the data set can be combined to form a high-resolution image. The number of images needed for reconstruction depends with the reconstruction algorithm used. For Vandewalle et al. [7], the optimal number of images used was six as this provided both balance in computation and resolution. However, there is a limit to the attainable improvements. Factors such as blur, noise and inaccuracies in the signal model limit the obtainable increase in resolution. It is important to note that an increase in the amount of pixels, does not necessarily suggest an increase in resolution. There are various studies that discuss different image reconstruction algorithms. However, for this paper, only three algorithms are discussed and implemented.

1) *Bicubic Interpolation*: For Vandewalle et al. [7], their image registration algorithm is partnered with a simple bicubic interpolation for their image reconstruction phase. Bicubic interpolation is performed by expressing the samples of the different low-resolution images in the coordinate frame of the reference image (usually the first low-resolution image generated) using the estimated registration parameters. From these known parameters, values of the low-resolution images are then interpolated in a high-resolution grid. The number of low-resolution images to be used depends on many parameters such as the registration accuracy, image model, total frequency content and the like.

2) *Projection Onto Convex Sets*: Patti et al. [4] proposed an algorithm using the theory of projections onto convex sets (POCS) to reconstruct super-resolution images. POCS requires the definition of closed convex constraint sets within a well-defined vector space that contains the actual high-resolution image. The high-resolution image estimate is defined as a point in the intersection of these constrained sets. This is determined by successively projecting an arbitrary initial estimate onto the constraint sets. Further discussion can be found in
[4] [6].

3) *Adaptive Normalized Convolution*: Pham et al. The algorithm proposed by [8] uses adaptive normalized convolution (NC) that works with LR images in an adaptive environment to create a corresponding high resolution image.

To do this, the algorithm first gathers the low resolution images and compares them to a common frame in order to adjust for pixel shift using a shift estimator [7][8], then robust fusion [8] using the adaptive NC is used

on the samples. After that, to reduce the blur and noise, a multi-frame deconvolution algorithm is used [8]. To further improve the resulting high-resolution image, it is first reconstructed by a locally weighted median operation, it is then used for the initial first-order robust NC [11] which produces an image and two derivatives which will be used to construct the applicability functions [8] for the last first-order adaptive NC. That way, the final NC will be much more suited to the situation in terms of structure, scale and sample size.

3. TESTS AND RESULTS

The image registration and image reconstruction algorithms were performed on four different data sets. The data sets are as follows: satellite images, images of craters from space, images of license plates from a distance of 10 meters, and x-ray images. The images from these data sets were downsampled by a factor of 4 and 5 other low-resolution images that have been rotated and shifted were generated. Gaussian zero-mean random variables are used for the shift (pixels) and rotation (degrees) parameters. For the shifts, a standard deviation of 2 is used, while the rotation angles have a standard deviation of 1. The different images were then passed through an ideal low-pass filter with a cut-off frequency $0.12u_s$where u_s is the sampling frequency of the image [7]. Thus, the tests conducted generated 6 low-resolution images from the original high-resolution image.

A. *Objective Testing*

Objective testing was done by downsampling the original high-resolution images into 6 low-resolution images with varying shifts and rotations. The low-resolution images were registered using [7] and reconstruction was done using the three image reconstruction algorithms: bicubic interpolation, POCS, and adaptive normalized convolution. The SNR of the resulting images of each algorithm was computed. This served as a simple method to evaluate the effectiveness of each algorithm for each data set. Images used in this study were placed in a separate appendix in order to avoid the bias in resizing the images.

1) *Satellite Imagery*: Two satellite images were acquired from [3] shown in Appendix A. From the resulting image registration and image reconstruction algorithms that were performed, the computed SNR for the three algorithms is shown in Table I.

TABLE I. SNR OF SATELLITE IMAGE SET

Algorithm	***Set 1***	***Set 2***
Bicubic Interpolation	2.9940	3.4484
POCS	2.0457	3.2993
Adaptive Normalized Convolution	2.5148	3.4590

TABLE II. SNR OF CRATER IMAGE SET

Algorithm	***Set 1***	***Set 2***
Bicubic Interpolation	6.8430	2.9173
POCS	8.1362	2.8740
Adaptive Normalized Convolution	6.5679	2.8445

The data set for this experiment, as shown in Appendix A, would suggest that bicubic interpolation experiences less noise than POCS or for the adapative normalized convolution. However, bicubic interpolation does not contribute to an increase in resolving power. For POCS and adaptive normalized convolution, the latter has a higher SNR than the former. Examining the results of the first satellite image set in Appendix A, all resulting images seem to suffer some form of blurring. Due to the amount of information present in the high-resolution image (varying pixels intensities that are compressed), reconstruction of the images results in an aliased image due to the Moire effect caused by insufficient sampling and the limitation of the reconstruction algorithms.

2) *Crater Images*: The two sets of images acquired from [1] are shown in Appendix A. The computed SNR is shown in Table II.

For this data set, POCS achieved the highest SNR. Closer inspection of the image in Appendix A, the resulting image from POCS is blurred. This can be accounted to the limitation of POCS. POCS does not account for the differing rotations in the low-resolution images. Examining the results of the adaptive normalized convolution, the produced image is comparatively sharper than POCS. Although POCS has a higher SNR than the adaptive normalized convolution algorithm, a higher SNR does not necessarily translate an image with a higher resolving power or resolution.

3) *X-Ray Images*: An x-ray image of a male and female patient were acquired from [DLSU Health Sciences] and shown in Appendix A. Table III. shows the computed SNR from the two sets of x-ray images.

TABLE III. SNR OF X-RAY IMAGE SET

Algorithm	***Set 1***	***Set 2***
Bicubic Interpolation	14.8702	11.9067
POCS	15.2174	12.7973
Adaptive Normalized Convolution	14.9904	11.9607

TABLE IV. SNR OF LICENSE PLATE IMAGE

Algorithm	***Set 1***
Bicubic Interpolation	15.5035
POCS	7.9442
Adaptive Normalized Convolution	15.3541

Text from the corners in the x-ray image is disregarded in this scenario since the main focus is on the lungs. POCS is once again the algorithm with the highest SNR, but the difference between the two other algorithms is not that significant. Due to an x-ray image being black and white, there are not much discernible differences in the generated output, and the blur in POCS is harder to detect.

4) *License Plate Detection*: A picture of an SUV was taken at a distance of approximately 10 meters. The goal of this test is to determine if the license plate can be comprehended after processing the low resolution images with the three image reconstruction algorithms. Appendix A shows the low-resolution image and the images generated from the reconstruction algorithms. Table IV. shows the SNR result from this test.

Among the three algorithms, POCS performed worst with an SNR of 7.94. This can be attributed to its lack of compensation for rotations in the image set. Appendix A shows the magnified version of the license plate after reconstructing the image using POCS. The blur caused by the inaccuracies produced by the rotation has made the license plate of the car indiscernible. However, certain letters from the license plate can still be observed. The algorithm generated some artifacts along the area of the license plate, and can be observed that compared with the original image, and the two other algorithms, the adaptive normalized convolution algorithms produced the best result based on SNR values.

B. Subjective Testing

Subjective testing was performed through a survey of 25 people. The respondents were asked to rank the resulting images from the previous test according to the image that matched the original high-resolution image the closest. A rank of 1 means that it is the closest image to the original, while a rank of 3 means it is the

farthest. The participants had no knowledge of which algorithm was used for each image set. The original high-resolution images were shown as well to form a basis for comparison.

1) *Satellite Imagery*: Figure 1 shows the average ranking of the two test images and the frequency of their ranks.

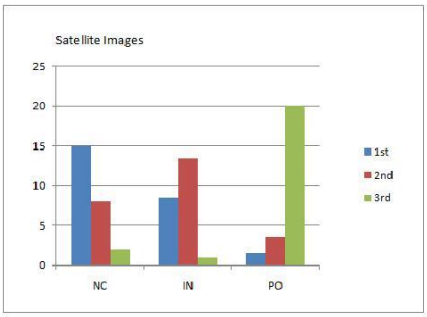

Figure 1. Averaged Frequency of Ranking for the Satellite Image Set

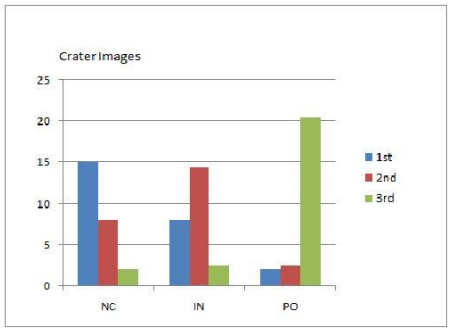

Figure 2. Averaged Frequency of Ranking for the Crater Image Set

The adaptive normalized convolution algorithm ranked first in the satellite image set followed closely by the bicubic interpolation. Among the three algorithms, it can be said that POCS ranked worst judging from the average frequency of the algorithm at third place.

2) *Crater Images*: For the set of crater images, it is apparent that the adaptive normalized convolution matched the original image better than the bicubic interpolation as suggested in Figure 2. Although POCS had the highest SNR ratio for this test, it can be inferred that it did not closely match the original image.

3) *X-Ray Images*: Most of the participants chose the image generated by the normalized convolution algorithm as the one that produced the best results. Consistent from the previous results, POCS is the one the participants ranked as the farthest from the original high-resolution image.

4) *License Plate Detection*: The participants in this test were asked to not only rank the image that closely matched the original test, but they were also asked to identify the license plate for image results of the bicubic interpolation, POCS, and the adaptive normalized convolution algorithm. Figure 4 confirms earlier observations that the image generated through POCS produces a noticeable blur in the image. All of the participants ranked the image generated by POCS as the farthest image from the original.

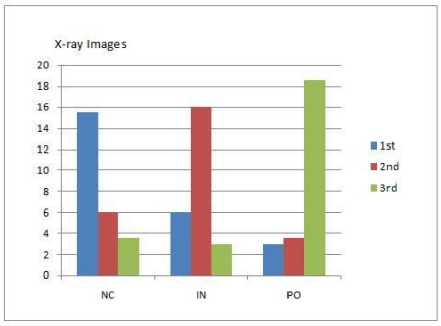

Figure 3. Averaged Frequency of Ranking for the X-Ray Image Set

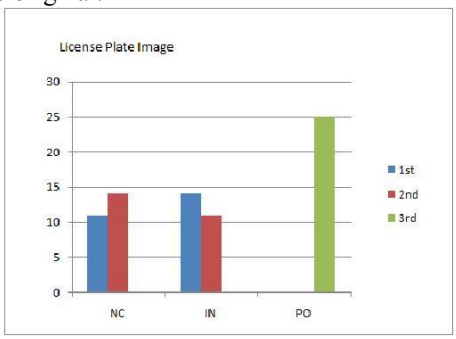

Figure 4. Averaged Frequency of Ranking for License Plate Determination

The difference in the image generated by bi-cubic interpolation and adaptive normalized convolution is not by much. However, more people ranked the interpolation algorithm as closer to the original image.

When asked to determine the license plate of the car, the POCS algorithm's result was undiscernible. Therefore the study did not ask the respondents to identify the license plate in the image generated by POCS.

The survey for this test was done in two parts. For the first part, the participants were asked to rank the image in the same way the previous tests were done. The second part of the test had a total of 50 participants. The first 25 participants were asked to identify the license plate in the image generated by the bicubic interpolation. The other 25 were asked to identify the image resulting from the adaptive normalized convolution algorithm. This was done to prevent one version of their interpretation from influencing the other. The participants would not have any prior knowledge of the image.

Accuracy for determining the license plate was determined by scoring the amount of letters the participant was able to distinguish. The scores of each participant were then averaged with everyone who took the survey. While the low-resolution image was unreadable, it was found that the bicubic interpolation yielded an accuracy of 68% and the adaptive normalized convolution was able to gain an accuracy of 80%.

4. ANALYSIS AND RECOMMENDATION

Vandewalle et al. [7] state that there is another challenge in super resolution. This challenge is to apply the information obtained from the multiple registered image sources to reconstruct a high-resolution image. This requires a nontrivial deconvolution operation in order to undo the blurring applied by a camera point spread function.

The POCS algorithm contains a low pass filter that approximates the point-spread function applied on the image; this is why its SNR is much higher as compared to the other results. However, this does not necessarily correspond to a better image in terms of quality and resolving power. This was made apparent by the results of the survey.

One possible reason why the adaptive normalized convolution algorithm scored higher on the subjective testing is because of the adaptive nature of the algorithm and its 2^{nd} pass processing phase, which makes the convolution performed more appropriate and creates a sharper image. However, a trade off for the increased sharpness is the time duration of image processing. The sharpness of the results from the adaptive normalized convolution algorithm may also produce artifacts that corrupt the image. This algorithm took approximately seven hours to process its image in Appendix A. The other two algorithms were able to process the images considerably faster compared to the adaptive normalized convolution algorithm. However the POCS result was incomprehensible and the interpolation result can be described as too smooth to determine the details completely and without difficulty.

There are many other super resolution algorithms not limited to deconstruction methods that may be deemed more appropriate than others for some image sets. According to the tests performed, none of these algorithms suit satellite imagery due to the compressed nature of the information in the images. This results in image aliasing. The algorithms produce an image with poorly estimated pixels.

These algorithms were found to work best for images that do not contain very precise details such as X-ray images. As for the crater images, upon closer inspection, some of the smaller edges and details were misaligned. However, precision depends on the amount of information needed. If only an estimate of the location is needed, then any of the algorithms would suffice.

For license plate detection, adaptive normalized convolution is preferred. However, a trade-off for increased information is a longer time-duration for processing. Even though the accuracy of the test was only 80%, car identification relies on several factors such as the type of car, colour and the like. The results in license plate detection can aid in applying constraints to the possible choices for identification. The generated image may produce possible license plate combinations, if not the correct combination itself. The results could then be cross-referenced with the other factors for car identification to find the needed vehicle. In other words, 80% accuracy would theoretically be enough for accurate license plate identification. However, more research is needed to optimize results.

Other super-resolution algorithms may be performed with these tests. Algorithms such as [10] use a single

image in order to construct a high-resolution image using patch redundancies in scaled down versions of the image to estimate some similar patches of the high resolution image. Super-resolution algorithms are not necessarily limited to image registration and image reconstruction algorithms. The gradient profiling algorithm [9] makes use of multiple gradient profiles of natural images to apply constraints on an image that is initially interpolated with conventional methods. However, further investigation must be done to verify their effectiveness in applications such as satellite imagery, space imaging, medical science and forensic analysis.

5. CONCLUSIONS

The algorithms presented in this paper were investigated in its applications to satellite imagery, space imaging, medical science, and forensic science. It was found that in terms of the SNR of each resulting image, the algorithms performed inadequately on satellite imagery but showed exceptional results on X-ray images. the algorithms performed the poorest in satellite imagery but performed well on X-ray images. The crater image set, although missing some of the sharper details, was deemed clear enough at first glance by the survey correspondents but may be deemed unacceptable for space exploration by satellite cameras.

Using an adaptive normalized convolution algorithm for image reconstruction yielded good results in determining the license plate of a car from an almost incomprehensible image. POCS was completely unable to recreate the plate number clearly while the bicubic interpolation yielded an accuracy of 68%. Judging from the results of the objective and subjective tests, it was discovered that a high SNR does not necessarily correspond to a higher resolving power. Further algorithms may still be used to verify their efficiency in the differing applications. A balance between processing time and image quality must also be considered.

6. ACKNOWLEDGEMENTS

The research group would like to thank Dr. Joel Ilao for his unending patience and strength of character in teaching his students. We also commend his excellence in the field of Machine Vision that guided the group in the course of this research. The group also extends their gratitude to Vandewalle for allowing the use of his open-source super-resolution software.

7. REFERENCES

[1] *Archimedes Crater*. (n.d.). Retrieved December 2012, from New York University Department of Mathematics: http://www.math.nyu.edu/~crorres/Archimedes/Crater/Crater.html.

[2] *Ikonos Satellite Image of Denver, Colorado*. (2012). Retrieved December 2012, from Satellite Imaging Corporation: http://www.satimagingcorp.com/gallery/ikonos-denver-lg.html.

[3] *Satellite*. (2011, July 18). Retrieved December 2012, from Maxwell Park Neighborhood Council: http://www.maxwellparknc.com/satellite.html.

[4] Patti, A. J., Sezan, M., & Tekalp, A. (1997, August). Super Resolution Video Reconstruction with Arbitrary Sampling Lattices and Non-zero Aperture Time. *IEEE Transactions on Image Processing, 6*(8), 1064-1076.

[5] Geaney, D. J. (2011, December 31). *Mars Travel: Mars Photo of the Day - Dec 31, 2011*. Retrieved December 2012, from Mars Travel: http://www.marstravel.org/2011/12/mars-photo-of-day-dec-31-2011.html.

[6] Dubois, E. (1985, April). The Sampling and Reconstruction of Time-Varying Imagery with

Application in Video Systems. *Proceedings of the IEEE, 73*(4), 502-522.

[7] Vandewalle, P., Süsstrunk, S., & Vetterli, M. (2005, May 18). A Frequency Domain Approach to Registration of Aliased Images with Application to Super-resolution. *EURASIP Journal on Applied Signal Processing, 2006*, 1-14.

[8] Pham, T. Q., Van Vliet, L. J., & Schutte, K. (2005, May 17). Robust Fusion of Irregularly Sampled Data using Adapative Normalized Convolution.

[9] Sun, J., Shum, H.-Y., & Xu, Z. (n.d.). Image Super-Resolution using Gradient Profile Prior. *Microsoft Research Asia.* Beijing. Retrieved from http://research.microsoft.com/en-us/um/people/jiansun/papers/GradientSR_CVPR08.pdf.

[10] Glasner, D., Bagon, S., & Irani, M. (n.d.). *Super Resolution from a Single Image.* Department of Computer Science and Applied Mathematics. Rehovot: The Weizmann Institute of Science.

[11] Knutsson, H., & Westin, C.-F. (n.d.). *Normalized and Differntial Convolution*. Sweden: Linkoping University.

APPENDIX A. IMAGES USED

TABLE 1. SATELLITE IMAGE 1 DESCRIPTIONS

Algorithm	***Original***	***Low Res***	***Processed***
Dimensions	1000x591	250x148	1000x591
Resolution	72dpi	72dpi	72dpi
Bit Depth	24	24	24

Figure 1-1. Satellite Image 1 – Sample Low-Resolution Image Generated

Figure 1-2. Satellite Image 1 – Interpolation Output

Figure 1-3. Satellite Image 1 – POCS Output

Figure 1-4. Satellite Image 1 – Normalized Convolution

TABLE 2. SATELLITE IMAGE 2 DESCRIPTIONS

Algorithm	***Original***	***Low Res***	***Processed***
Dimensions	720x720	180x180	720x720
Resolution	72dpi	72dpi	72dpi
Bit Depth	24	24	24

Figure 2-1. Satellite Image 2 – Sample Low-Resolution Image Generated

Figure 2-1. Satellite Image 2 – Sample Low-Resolution Image Generated

Figure 2-2. Satellite Image 2 – Interpolation Output

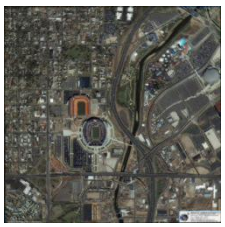

Figure 2-3. Satellite Image 2 – POCS Output

Figure 2-4. Satellite Image 2 – Normalized Convolution Output

TABLE 3. CRATER IMAGE 1 DESCRIPTIONS

Algorithm	***Original***	***Low Res***	***Processed***
Dimensions	1000x562	250x141	1000x562
Resolution	72dpi	72dpi	72dpi
Bit Depth	24	24	24

Figure 3-1. Crater 1 – Sample Low-resolution Image Generated

Figure 3-2. Crater 1 – Interpolation Output

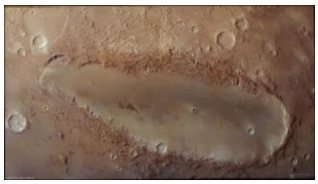

Figure 3-3. Crater 1 – POCS Output

Figure 3-4. Crater 4 – Normalized Convolution

TABLE 4. CRATER IMAGE 2 DESCRIPTIONS

Algorithm	***Original***	***Low Res***	***Processed***
Dimensions	840x1000	210x250	840x1000
Resolution	72dpi	72dpi	72dpi
Bit Depth	8	8	8

Figure 4-1. Crater 2 – Sample Low-resolution Image Generated

Figure 4-2. Crater 2 – Interpolation Output

Figure 4-3. Crater 2 – POCS Output

Figure 4-4. Crater 2 – Normalized Convolution Output

TABLE 5. XRAY IMAGES DESCRIPTIONS

Figure 5-1. Xray 1 – Sample Low-resolution Image Generated

Figure 5-2. Xray 1 – Interpolation Output

Figure 5-3. Xray 1 – POCS Output

Figure 5-4. Xray 1 – Normalized Convolution Output

Figure 6-1. Xray 2 – Sample Low-resolution Image Generated

Figure 6-2. Xray 2 – Interpolation Output

Figure 6-3. Xray 2 – POCS Output

Algorithm	***Original***	***Low Res***	***Processed***
Dimensions	557x680	140x170	557x680
Resolution	96dpi	72dpi	72dpi
Bit Depth	24	24	24

Figure 6-4. Xray 2 – Normalized Convolution Output

TABLE 6. LICENSE PLATE IMAGE DESCRIPTIONS

Algorithm	***Original***	***Low Res***	***Processed***
Dimensions	2592x1944	648x486	2592x1944
Resolution	72dpi	72dpi	72dpi
Bit Depth	24	24	24

Figure 7-1. License Plate – Sample Low-resolution Image Generated

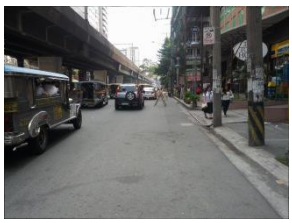

Figure 7-2. License Plate – Interpolation Output

Figure 7-3. License Plate – POCS Output

Figure 7-4. License Plate – Normalized Convolution Output